BioSystems 101 (2010) 149–155

Contents lists available at ScienceDirect

BioSystems

journal homepage: www.elsevier.com/locate/biosystems

# First order phase transition and hysteresis in a cell's maintenance of the membrane potential—An essential role for the inward potassium rectifiers

Jill Gallaher[a,**], Martin Bier[a,*], Jan Siegenbeek van Heukelom[b]

[a] Dept. of Physics, East Carolina University, Greenville, NC 27858, USA
[b] Swammerdam Institute for Life Sciences, Center for Neurosciences, University of Amsterdam, Amsterdam, The Netherlands

ARTICLE INFO

*Article history:*
Received 22 February 2010
Received in revised form 28 May 2010
Accepted 31 May 2010

*PACS:*
87.16.dp
64.70.qj
87.15.ad
87.15.Zg

*Keywords:*
Inward rectification
Hypokalemia
Hysteresis
Phase transition
Transmembrane potential

ABSTRACT

Hysteretic behavior is found experimentally in the transmembrane potential at low extracellular potassium in mouse lumbrical muscle cells. Adding isoprenaline to the external medium eliminates the bistable, hysteretic region. The system can be modeled mathematically and understood analytically with and without isoprenaline. Inward rectifying potassium channels appear to be essential for the bistability. Relations are derived to express the dimensions of the bistable area in terms of system parameters. The selective advantage and evolutionary origin of inward rectifying channels and hysteretic behavior is discussed.



## 1. Introduction

Biological switches are as common as they are diverse. Quantitative accounts of such switches in terms of basic physics and chemistry are often reminiscent of the way traditional physics has dealt with phase transitions (Plischke and Bergersen, 1994; Reichl, 1980). Getting a discrete switch in a system with underlying continuous dynamics involves bifurcations, i.e., solutions that emerge and disappear as a parameter is changed. Such bifurcations have been identified in population dynamics and in signaling pathways that involve DNA and/or proteins (Edelstein-Keshet, 1988; Murray, 1993; Ferrell and Machleder, 1998; Qian and Reluga, 2005). An adverse environment may trigger the "switching off" of activity as in the case of dormancy of persister cells (Lewis, 2007) or sporulation of yeast (Sonenshein, 2000). Environmental stress can be the cause for many cells and organisms to retreat from activity until conditions are more energetically favorable for proliferation (Wharton, 2002).

Cells are sensitive to external potassium concentration changes. For potassium the transmembrane electric potential and the transmembrane chemical potential almost balance each other out. Under physiological conditions a large fraction of the potassium channels is open which helps stabilize the electric potential. Too much potassium (hyperkalemia) in the medium can cause depolarization of the transmembrane potential. With too little potassium in the medium (hypokalemia) a more complicated situation arises. As the concentration of extracellular potassium lowers, the membrane becomes hyperpolarized. Beyond a certain threshold, a switch to a depolarized state is observed to occur in a variety of cell types (Gadsby and Cranefield, 1977; McCullough et al., 1990; Siegenbeek van Heukelom, 1991; Brismar and Collins, 1993; Jiang et al., 2001). This transition appears reversible as potassium is added again to the extracellular medium. However, the switch back to a hyperpolarized state occurs at a higher potassium concentration than the one for which to depolarization occurred. There is an apparent hysteresis. In our previous works we have shown that these switches do not go via the genome (van Mil et al., 2003; Geukes Foppen and Siegenbeek van Heukelom, 2003; Gallaher et al., 2009). A very simple model, involving only sodium channels, potassium channels, and Na,K-ATPase pumps, can quantitatively account for the bistable behavior.

Inward rectifying potassium channels (IRKs) appear to be essential for the bistable behavior. When the electrochemical potential

* Corresponding author.
** Principal corresponding author.
*E-mail addresses:* jag0504@ecu.edu (J. Gallaher), bierm@ecu.edu (M. Bier), jsvhviii@hetnet.nl (J.S. van Heukelom).

0303-2647/$ – see front matter © 2010 Elsevier Ireland Ltd. All rights reserved.
doi:10.1016/j.biosystems.2010.05.007

for potassium is such that too much potassium is driven outward, the IRKs close. This characteristic results in a kind of "protection" of the high intracellular potassium concentration (which, under physiological conditions, is about twenty times as high as the extracellular concentration) and this is often thought to be the reason that IRK properties first evolved more than 2.4 billion years ago (Hille, 1992). The dynamics of the system of pumps and channels is such that the closing of a small fraction of IRK channels leads to the closing of more IRK channels (Goodman and Art, 1996; Lu, 2004). Because of this positive feedback mechanism there are no continuous transitions between the hyperpolarized and the depolarized state. Instead it is found, theoretically and experimentally, that there is a genuine non-equilibrium first order phase transition (Moore, 1972). It is furthermore found that, in a certain value range of the extracellular potassium concentration, both the hyperpolarized state and the depolarized state are stable and hysteretic behavior occurs (Jackson, 1989). This bistable region is only slightly below the physiological concentration of extracellular potassium and may be easily encountered.

Below we will first present the result of experiments in which we dramatically increased the potassium permeability, $P_K$, of the cell membrane. We do so by adding isoprenaline to the medium. The dependence on concentration and electric potential of the IRK's open-closed behavior will be overwhelmed and become negligible in this case. With this fixed, constant and high $P_K$ we find that the phase transition and the bistability no longer occur. It is furthermore found that for the case of high constant $P_K$ an analytic solution can be found for the steady state equations for the sodium and potassium flow. Theory and experiment appear in very good agreement. We also compare the isoprenaline case with the control in which the $P_K$ is dominated by IRKs.

The hypophysiological concentration of extracellular potassium leads to a larger outbound force on intracellular potassium. A hyperpolarization can compensate for this increased chemical force. However, such hyperpolarization implies a larger leak of sodium ions and a concurrent increased demand on the Na,K-ATPase pumps. At some point, the hyperpolarization may simply become too metabolically costly to maintain. What we will see is that, with the variable $P_K$ of the IRKs, a radical switch from the hyperpolarized branch to a depolarized branch occurs at some value of the extracellular potassium concentration. In the depolarized state the potassium channels are largely closed and the sodium leak is decreased. By blocking ion flow and ceasing the metabolic efforts that maintaining such flow requires, the cell effectively isolates itself from the adverse environment and "goes into hibernation." We see that upon again increasing the extracellular potassium concentration, $K_e$, a switch back to the hyperpolarized state occurs. However, as was mentioned before, that switch back to the hyperpolarized branch occurs at a $K_e$ that is about half a millimolar higher than the $K_e$ at which the switch to the depolarized branch occurs. So, only when the environment is well within the "healthy" domain does the cell "wake up" again.

It is likely that the bistability evolved as a functional response to environmental adversity. In the discussion section we will speculate on the survival value of the cell's bistability.

## 2. The Model

A potential difference across the cell's membrane is necessary for survival. Muscle cells have a transmembrane potential of around −75 mV inside to outside at normal physiological conditions. The prominent ions, sodium and potassium, are pumped against the electrochemical potential by the ATP driven Na,K-ATPase in order to maintain a high potassium concentration and a low sodium concentration inside the cell. Our model involves only the Na,K-ATPase, sodium channels, and potassium channels. Despite neglecting all other ions and transporters, remarkable accuracy will be obtained.

At steady state there is, for each ion, an equal and opposite passive flow through ion channels. To model the flux of ions across the cell membrane, we have the following steady state equations:

$$P_{Na}U\frac{N_i - N_e e^{-U}}{1-e^{-U}} = -3k_p\mu(K_e;K_m^K)\mu(N_i;K_m^N) \quad (1)$$

$$P_K U\frac{K_i - K_e e^{-U}}{1-e^{-U}} = 2k_p\mu(K_e;K_m^K)\mu(N_i;K_m^N). \quad (2)$$

For both sodium (Eq. (1)) and potassium (Eq. (2)) these equations describe how the leak (on the left hand sides) must equal the active transport (on the right hand sides). $P_{Na}$ and $P_K$ represent the membrane permeabilities for sodium and potassium and these are multiplied with the electrochemical potentials for the respective ions to obtain the leak rate. Here $U$ represents a dedimensionalized form of the electric transmembrane potential ($V_m$): $U = eV_m/(k_BT)$, where $e$ is the elementary charge, $k_B$ is the Boltzmann constant, and $T$ is the temperature in degrees Kelvin. The constant $e/(k_BT)$ equals $38\,V^{-1}$ at $T = 300\,K$. $N_i$ and $K_i$ represent the intracellular sodium and potassium concentrations. $N_e$ and $K_e$ represent the extracellular concentrations of sodium and potassium. The leak described on the left hand side of (1) and (2) is compensated for by the activity of the Na,K-ATPase, the sodium-potassium pump. For every cycle the Na,K-ATPase brings three sodium ions from the inside to the outside and two potassium ions from the outside to the inside. The pump activity is described with rate-limiting Michaelis–Menten kinetics in both the extracellular potassium concentration and the intracellular sodium concentration. $k_p$ is the maximal turnover rate for the pump and $\mu(x;K_m^x) = x/(K_m^x + x)$. The textbook by Läuger gives $K_m^K = 0.2$ mM and $K_m^N = 0.6$ mM, which were experimentally determined using red blood cells (Läuger, 1991). The 0.2 mM represents the extracellular potassium concentration that, with saturating intracellular sodium concentration, leads to a half-maximal turnover rate for the pump. Likewise, 0.6 mM represents the intracellular sodium concentration that, with a saturating extracellular potassium concentration, leads to a half-maximal turnover rate for the pump.

The potential difference $U$ comes about as a consequence of sub-micromolar differences in concentration between cations and anions. In this model sodium and potassium are the only permeable ions. The concentrations of sodium and potassium are all millimolar or higher. We therefore work with an electroneutrality condition:

$$N_i - N_e = -(K_i - K_e) = \delta C. \quad (3)$$

The variable $\delta C$ denotes the chemical imbalance between the cell and the medium in which it is immersed. Eq. (3) also imposes an osmotic balance ($N_i + K_i = N_e + K_e = C$) requiring that the total concentration of permeable solutes is equal in the extracellular and the intracellular solution. The model we have set up here uses the notation of Keener and Sneyd (1998).

With Eqs. (1)–(3) we have three equations with three unknowns ($N_i$, $K_i$, and $U$). By separating out the quotients on the left hand side and adding up Eqs. (1) and (2) we obtain a single expression for $U$ in which the exponentials have canceled:

$$U = -\left(\frac{3k_p}{N_e+K_e}\right)\left(\frac{P_K - (2/3)P_{Na}}{P_K P_{Na}}\right)\left(\frac{K_e}{K_m^K+K_e}\right)\left(\frac{N_i}{K_m^N+N_i}\right). \quad (4)$$

This may look straightforward until one considers the nature of $P_K$. For the IRK channels, $P_K$ depends on the electrochemical potential of potassium, i.e., on $K_e$, $K_i$, and $U$. To better understand the system we will first explore, theoretically and experimentally, what happens when $P_K$ is constant and much larger than $P_{Na}$. We can accomplish this by adding isoprenaline to the medium.

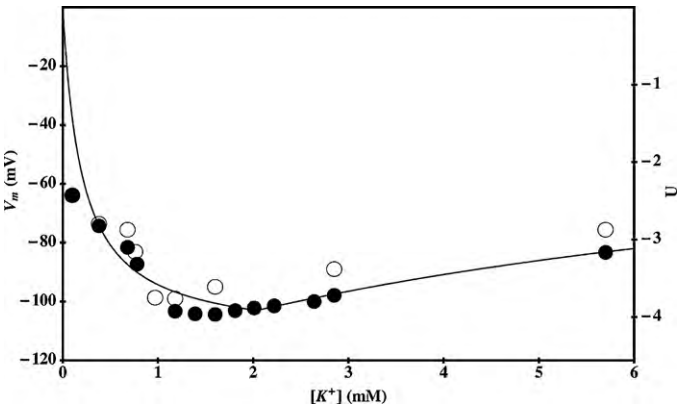


**Fig. 1.** The dots represent experimental data taken at $N_e + K_e = 0.15$ M with 1 μM isoprenaline in the medium. The filled dots represent the voltage after relaxation (about 5 min) as $K_e$ is decreased in a stepwise fashion. The open circles represent the voltages as $K_e$ is increased again. The theoretical curve is according to Eq. (9) with $K_m^K = 0.2$ mM, $3k_p/P_{Na} = 0.65$ M.

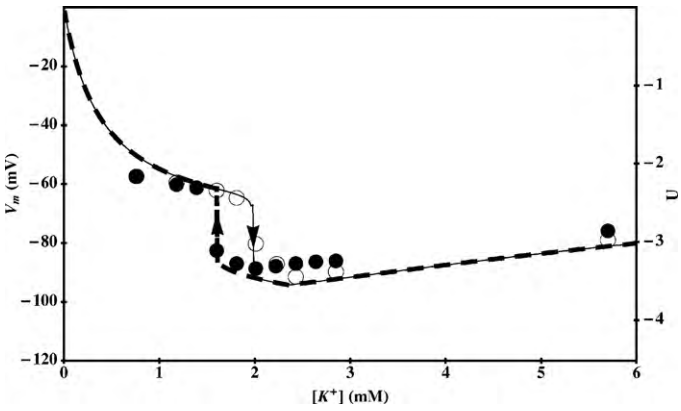


**Fig. 2.** The dots represent experimental data for the control situation taken at $N_e + K_e = 0.15$ M. The filled dots represent the voltage after relaxation as $K_e$ is decreased in a stepwise fashion. The open circles represent the voltages as $K_e$ is increased again. The theoretical curve is found by solving for $U$ by Eq. (11) numerically stepwise using a Newton scheme at each $K_e$. It is thick and dashed for decreasing $K_e$ and thin and continuous for increasing $K_e$. The parameters used were $P_{Na} = 5.4 \times 10^{-9}$ dm/s, $P_0 = 1.1 \times 10^{-8}$ dm/s, $P_{IRK}^{max} = 9.6 \times 10^{-8}$ dm/s, $\tilde{U} = 1.3$, $\varepsilon = 0.12$, $K_m^K = 0.40$ mM, and $U_{max} = -4.3$.

## 3. Isoprenaline Eliminates Bistability

Isoprenaline is a slowly hydrolyzable beta adrenergic agonist. Pharmacologically it has been utilized to increase the heart rate and relax the airways to increase air flow. Isoprenaline closes IRKs (Geukes Foppen et al., 2003), but the characteristic of isoprenaline that is important in this section is the ability to open $Ca^{2+}$-gated potassium channels (Kume et al., 1989). The number of such channels in the muscle cells that we study is very large (Sejersted and Sjøgaard, 2000; Kristensen et al., 2006). The permeability associated with the $Ca^{2+}$-gated potassium channels far overwhelms the permeability due to IRKs. The opening results in a $P_K$ that is large and independent of $K_e$, $K_i$, and $U$.

In our experiments we measured the transmembrane potential of superficial cells of the lumbrical muscle of the mouse *in vitro*. Cells were impaled with fine tipped glass microelectrodes and remained in the cell for the entire duration of the experiment. Ion concentrations in the extracellular medium were under our control and the temperature was maintained at 35 °C. We first let the cell come to a steady state with the physiological value $K_e = 5.7$ mM and we then measure $U$. As $K_e$ was changed in a stepwise fashion, the osmolarity of the external medium was kept constant, i.e. $N_e + K_e = C$. After each time that $K_e$ was changed, the system was given sufficient time to reach the new steady state before the voltage was recorded. A more detailed account of the procedures can be found in the references (Siegenbeek van Heukelom, 1991; van Mil et al., 1997, 2003; Geukes Foppen, 2004). Figs. 1 and 2 were obtained on the same cell. They show results with and without isoprenaline added to the external bath. The closed circles in Figs. 1 and 2 show the measured $U$'s of the cells as $K_e$ was decreased in small steps. The open circles represent the voltages $U$ as $K_e$ is increased again. Throughout our experiments the [ATP]/([ADP][P]) ratio is buffered at a saturating level and it therefore is not a factor.

Adding isoprenaline to the external solution results in a situation with $P_{Na} \ll P_K$ by between one and two orders of magnitude. Using this and the $N_e + K_e = C$ condition, we approximate Eq. (4):

$$U = -\frac{3k_p}{P_{Na}C}\left(\frac{K_e}{K_m^K + K_e}\right)\left(\frac{N_i}{K_m^N + N_i}\right). \tag{5}$$

The right hand sides of Eqs. (1) and (2) are of the same order of magnitude, but on the respective left hand sides $P_K$ is about two orders of magnitude larger than $P_{Na}$. It is for this reason that the electrochemical potential for sodium (with $N_i - N_e \exp[-U]$ in the numerator) is two orders of magnitude larger than the one for potassium (with $K_i - K_e \exp[-U]$ in the numerator). If we take $K_i = K_e \exp[-U]$, we get $N_i = C - K_e \exp[-U]$. Substituting this in (5) we find after some algebra:

$$U = -\frac{3k_p}{P_{Na}C}\left(\frac{K_e}{K_m^K + K_e}\right)\left(1 + \frac{K_m^N}{C - K_e e^{-U}}\right)^{-1}. \tag{6}$$

This is a relation between $K_e$, $U$, and a number of constant parameters. With a further approximation it is possible to obtain an explicit and simple expression for $U$ as a function of $K_e$. In the regime where $K_e$ is larger than about 2 mM, we take the $K_e/(K_m^K + K_e)$ to be one. We then have a relation

$$U = U_{max}\left(1 + \frac{K_m^N}{C - K_e e^{-U}}\right)^{-1}, \tag{7}$$

where $U_{max} = -3k_p/(P_{Na}C)$. Solving for $K_e$ we find

$$K_e = e^U\left(C + K_m^N \frac{U}{U - U_{max}}\right). \tag{8}$$

$C$ is larger than $K_m^N$ by a factor of about 250. So $U = \ln[K_e/C]$ is a good approximation until $U$ comes very close to $U_{max}$.

In a $U$ vs. $K_e$ graph we have a decrease of $U$ (following $U = \ln[K_e/C]$) as $K_e$ decreases. But as $K_e$ approaches 2 mM and $U$ approaches $U_{max}$, a horizontal asymptote at $U = U_{max}$ is approached from above. Thus when $K_e$ gets very low this approximation will not hold. However going back to Eq. (5), at low $K_e$ the sodium flux increases making $N_i$ much greater than $K_m^N$ so that the last term goes to unity. We then end up with the following concise expression for $U(K_e)$:

$$U(K_e) = \begin{cases} \ln\left(\dfrac{K_e}{C}\right)\dfrac{K_e}{K_m^K + K_e}, & \text{if } K_e > K_e^* \\ U_{max}\dfrac{K_e}{K_m^K + K_e}, & \text{if } K_e < K_e^*. \end{cases} \tag{9}$$

In order to connect the two parts of this curve at $K_e = K_e^*$ we need $U_{max} = \ln[K_e^*/C]$. Fig. 1 shows the data points deriving from the experiment together with a fit obtained with $K_m^K = 0.2$ mM and $K_e^* = 2$ mM. The latter value leads to $U_{max} = -4.3$, which, in terms of Volts, corresponds to −110 mV. In the experiments we kept $N_e + K_e = C$ at 150 mM and this value was used in Eq. (9) to obtain the fit.

When $U_{max} = -4.3$ is related back to the expression $U_{max} = -3k_p/(P_{Na}C)$ we find $3k_p/P_{Na} = 0.65$ M. This is in good agreement

with some independent estimates of $k_p$ and $P_{Na}$. The reference by Sejersted (1988) gives 50 pmole $s^{-1}$ $cm^{-2}$ for the steady-state, transmembrane flux of sodium ions of a muscle cell in physiological conditions. We use this for $3k_p$. Molar (M) is mole per liter, i.e., mole per cubic decimeter. For consistency we convert to decimeter (dm) for our unit of distance. We then have $3k_p = 5 \times 10^{-9}$ mole $s^{-1}$ $dm^{-2}$. The reference by Costa et al. (1989) reports $P_{Na} = 5.4 \times 10^{-9}$ dm/s for *Xenopus laevis* oocytes. Combination of the data of Sejersted and Costa et al. data gives 0.9 M for $3k_p/P_{Na}$. This is reasonably close to our 0.65 M. Fig. 1, moreover, shows a very good agreement between Eq. (9) and the experimentally recorded membrane potentials.

## 4. IRKs Produce Bistability

The IRK channel has an open probability that depends on the transmembrane potential as well as on intracellular and extracellular potassium concentrations (Hagiwara and Takahashi, 1974; Standen and Stanfield, 1978). The dependence appears to be well approximated by one on just the net electrochemical potential of potassium, i.e., $U - \ln(K_e/K_i)$ (Lu, 2004). It was, furthermore, observed already decades ago by Katz that current through the IRK decreased when $K_e$ was decreased (Katz, 1949). It is not difficult to understand how the membrane potential can affect the open probability. A membrane potential of about 100 mV leads to a huge electric field inside the membrane (which is only about 5 nm thick). As that field changes, charged groups in or near the lining of the channel can reposition and thus modulate a channel's conductivity. How actual ion concentrations can affect a channel's conductivity is still a subject of active research (Guo and Lu, 2003; Yan et al., 2005). The current versus voltage relationship has been fit many times to a Boltzmann distribution (Yang et al., 1995; Stadnicka et al., 2000; Lu, 2004; Struyk and Cannon, 2008). We summarize and approximate the potassium permeability with the following empirically based formula:

$$P_K = P_0 + P_{IRK}^{max}\left\{1 + \exp\left[\frac{1}{\varepsilon}\left(U - \ln\left(\frac{K_e}{K_i}\right) - \tilde{U}\right)\right]\right\}^{-1}. \quad (10)$$

$P_0$ represents the part of the potassium permeability that does not involve the IRKs and $P_{IRK}^{max}$ is the maximum permeability of IRKs only. The inverse of the term in curly brackets is a Boltzmann distribution for the open fraction of the IRKs. The fraction of channels that is open depends on the net electrochemical potential of potassium ($U - \ln(K_e/K_i)$) and the parameters $\tilde{U}$ and $\varepsilon$. For $U - \ln(K_e/K_i) = \tilde{U}$ the open-closed distribution is fifty–fifty. The small positive value of $\tilde{U}$ ($\tilde{U} \approx 1.3$, corresponding to about 30 mV) guarantees that the IRKs are mostly open when the net electrochemical potential of potassium is about zero. Some versions of Eq. (10) include a prefactor that depends on the potassium concentration (Sims et al., 1991; Siegenbeek van Heukelom, 1994; Goodman and Art, 1996; Liu et al., 1998; van Mil et al., 2003; Gallaher et al., 2009), but we have left that out, as within our range of interest that dependence is negligible compared to the exponential dependence in the Boltzmann expression.

The $P_K$ vs. $U$ curve has a sigmoidal shape. For $U - \ln(K_e/K_i) \ll \tilde{U}$, the asymptotic value is $P_K = P_0 + P_{IRK}^{max}$ and the potential is hyperpolarized. For $U - \ln(K_e/K_i) \gg \tilde{U}$, the asymptotic value is $P_K = P_0$ and the potential is depolarized. The parameter $\varepsilon$ gives the sensitivity of the open-closed distribution to the modified electrochemical potential $U - \ln(K_e/K_i) - \tilde{U}$. A small value of $\varepsilon$ leads to a steep and sharp transition between the hyperpolarized and depolarized limits.

We explore, theoretically and experimentally, the regime where $K_e$ is taken to below the physiological value of about 5.7 mM. In the last section we saw that for $K_e > K_e^*$ we have $U \approx \ln(K_e/C)$. In that case we have $P_K \gg P_{Na}$ and we find ourselves on the branch described on the first line of Eq. (9). It is obvious from Eq. (9) that once we cross over into the regime $K_e < K_e^*$, we have $U(K_e) > \ln(K_e/C)$. This means that the transmembrane electric potential for potassium and the chemical potential for potassium are no longer balancing each other out. A situation with most of the IRKs being open can then no longer be maintained. With $P_0$ for $P_K$, we have a $P_K$ that is of the same order of magnitude as $P_{Na}$. We can therefore no longer work with Eq. (5) and have to go back to Eq. (4). With $P_0$ and $P_{Na}$ of the same order of magnitude, the factor $(P_K - (2/3)P_{Na})$ will significantly differ from $P_K$. With a small $K_e$ we also have $N_i \gg K_m^N$. These conditions lead to a new condition for small $K_e$ that incorporates the bistability. All in all, we have for the two branches:

$$U(K_e) = \begin{cases} \ln\left(\dfrac{K_e}{C}\right)\dfrac{K_e}{K_m^K + K_e}, & \text{if } K_e > K_e^* \\ U_{max}\left(1 - \dfrac{2}{3}\dfrac{P_{Na}}{P_K}\right)\dfrac{K_e}{K_m^K + K_e}, & \text{if } K_e < K_e^*. \end{cases} \quad (11)$$

In order to connect the two parts of the curve we assume that the bistable region is within the low $K_e$ regime so that $\ln(K_e^*/C) = U_{max}(1 - (2/3)(P_{Na}/(P_0 + P_{IRK}^{max})))$. The $K_e^*$ is higher in the control (Eq. (11)) than in the isoprenaline case (Eq. (9)) because the term $(1 - (2/3)(P_{Na}/(P_0 + P_{IRK}^{max})))$ drops slightly below unity. Fig. 2 shows the results of experiments together with curves derived from the modeling.

With the IRKs, the closing of a small fraction of channels can lead to a snowball effect that does not occur with the constant $P_K$ of the last section. The increase in $U$ that follows the closing of a small fraction of IRKs leads to an increase of the term in curly brackets in Eq. (10). This implies a decrease of $P_K$. The smaller $P_K$, in turn, will drive the membrane potential $U$ further away from $\ln(K_e/K_i)$ and closer to $\ln(N_e/N_i)$, i.e., $U$ will increase faster, leading to a further decrease in $P_K$, etc. The "snowball" will stop when all IRKs are closed. With $P_K = P_0$ we are then on the depolarized branch. We take $K_e = K_e^{h\to d}$ for the extracellular potassium concentration at which we switch from the hyperpolarized branch to the depolarized branch.

A similar snowball effect takes place once we are on the depolarized branch (cf. Fig. 2) and we start increasing $K_e$ again. Opening of a small fraction of IRKs can lead to hyperpolarization, i.e., $U$ goes down. But a $U$ that is further decreasing into the negative regime will increase $P_K$ (cf. Eq. (10)). In this case the "snowball" will stop once all IRKs are open and $P_K = P_0 + P_{IRK}^{max}$. This switch occurs at $K_e = K_e^{d\to h}$.

## 5. The Dimensions of the Bistable Area

We start this section by focusing in on the bistable area (cf. Fig. 3) and applying a very rough approximation. The approximation is based on the following *Ansatz*. Going from the hyperpolarized branch to the depolarized branch, the aforementioned snowballing to the depolarized branch will occur after about *half* of the IRKs have closed. Likewise, the snowball effect leading to the massive opening in the depolarized-to-hyperpolarized transition will start after about *half* of the channels have already opened. It is possible to use a fraction different from 1/2. It is also possible to use different fractions for the two transitions. However, with a factor of 1/2 there is a plausible symmetry between the two transitions. The fraction of 1/2 means that the argument of the exponent in Eq. (10) equals zero. The *Ansatz* thus leads to:

$$U_{hyp} - \ln\left(\frac{K_e^{h\to d}}{K_i}\right) - \tilde{U} \approx U_{dep} - \ln\left(\frac{K_e^{d\to h}}{K_i}\right) - \tilde{U} \approx 0. \quad (12)$$

In Eq. (12) we observe that the bistable area can be shifted to lower $K_e$-ranges by increasing $\tilde{U}$. Mathematically with Eq. (12) it is also possible to compensate for an increased $\tilde{U}$ by increasing $U_{hyp}$

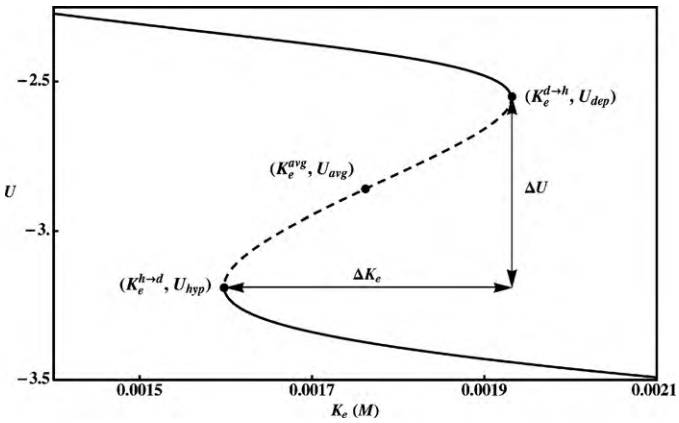


**Fig. 3.** A close-up view of the same theoretical curve of Fig. 2 with the points of interest highlighted. Just the second part of Eq. (11), where the bistability is present, is shown here. The stable solutions are represented with a solid line and the unstable region is represented with a dashed line. The points of switching, the center inflection point, and the height and width are all labelled with the notation that is found in the text.

and $U_{dep}$. However, the value of $U_{hyp}$ is tied to $U_{\max}$ and it is largely fixed by the mechanisms that were identified in Sections 3 and 4 and resulted in Eqs. (9) and (11). In numerical simulations of the system it is indeed observed that changing $\tilde{U}$ leads to a horizontal shift of the bistable area (Siegenbeek van Heukelom, 1994; van Mil et al., 2003; Gallaher et al., 2009). With these equations we can derive relations between and estimates for $U_{hyp}$, $U_{dep}$, $K_e^{h\to d}$, and $K_e^{d\to h}$.

The intracellular potassium concentration $K_i$ is supposed not to change too much as the switch occurs. After all, the entire point of the bistability appears to be the protection of the high $K_i$. From Eq. (12) we derive the following formula for the magnitude of the switch:

$$\Delta U = U_{dep} - U_{hyp} \approx \ln\left(\frac{K_e^{d\to h}}{K_e^{h\to d}}\right). \tag{13}$$

From Eq. (13) we take advantage of the apparent symmetry and assume that the switch points are equidistant from a central point (i.e., $K_e^{avg} = K_e^{d\to h} - \Delta K_e/2 = K_e^{h\to d} + \Delta K_e/2$). With a small $\Delta K_e$ we can use the fact that $\ln(1+\delta) \approx \delta$ for $\delta$ close to zero. We can then actually derive a linear relationship between the magnitude of the height ($\Delta U$), the width ($\Delta K_e = K_e^{d\to h} - K_e^{h\to d}$), and the center ($K_e^{avg}$) of the bistable area:

$$\Delta U \approx \left(\frac{\Delta K_e}{K_e^{avg}}\right). \tag{14}$$

In Fig. 3 we observe that $K_e^{h\to d} \approx 1.6$ mM and $K_e^{d\to h} \approx 1.95$ mM. These values in Eq. (13) predict $\Delta U \approx 0.20$. From Fig. 3 the two branches appear to be separated by $\Delta U = 0.65$ or about 17 mV. The *Ansatz* apparently leads to an estimation of the right order of magnitude. However, refinement is possible.

The term $\{1 + \exp[(U - \ln(K_e/K_i) - \tilde{U})/\varepsilon]\}^{-1}$ in the expression for the $P_K$ describes a sigmoid that, as $(U - \ln(K_e/K_i))$ increases, goes from an asymptotic value of 1 to an asymptotic value of 0. The transition from 1 to 0 is steeper if the value for $\varepsilon$ is smaller. In the $\varepsilon \to 0$ limit, it no longer matters whether we take 1/2 or any other number between 0 and 1 as the critical fraction at which the "snowballing" starts. In case of $\varepsilon \to 0$, we can also use different fractions for the two transitions without affecting the result. This is because with $\varepsilon \to 0$ the transition from 0 to 1 is effectively vertical. The experimental data in Fig. 2 were best fit with $\varepsilon = 0.12$. We observed that around that value for $\varepsilon$ we can still vary the width of the bistable area by varying $\varepsilon$. This means that with $\varepsilon = 0.12$ we are not yet in the regime where the $\varepsilon \to 0$ limit applies and the fractions may vary from 1/2.

We can obtain equations for the turning points because the tangent line to the theoretical curve in Fig. 3 becomes vertical when the switching occurs. Using the second part of Eq. (11) with $\partial U/\partial K_e \to \infty$ leads to two equations, one for $U_{dep}$ and one for $U_{hyp}$:

$$U_{dep} - \tilde{U} - \ln\left(\frac{K_e}{K_i}\right) = \varepsilon \ln\left(\frac{P_0 + P_{\mathrm{IRK}}^{\max}}{P_0}\right) + \varepsilon \operatorname{arccosh}(-G(K_e)) \tag{15}$$

$$U_{hyp} - \tilde{U} - \ln\left(\frac{K_e}{K_i}\right) = \varepsilon \ln\left(\frac{P_0 + P_{\mathrm{IRK}}^{\max}}{P_0}\right) - \varepsilon \operatorname{arccosh}(-G(K_e)), \tag{16}$$

where

$$G(K_e) = 1 + \frac{U_{\max} P_{\mathrm{Na}} P_{\mathrm{IRK}}^{\max}}{3\varepsilon P_0 (P_0 + P_{\mathrm{IRK}}^{\max})} \frac{K_e}{K_e + K_m^K}. \tag{17}$$

The symmetry is easy to see along the $U$-axis as the term $\varepsilon \operatorname{arccosh}(-G(K_e))$ on the right hand sides of Eqs. (15) and (16) shifts the potential up or down from a central point $\varepsilon \ln((P_0 + P_{\mathrm{IRK}}^{\max})/P_0)$ by nearly equal amounts ($K_e$'s are slightly different). In fact, getting rid of the last term on the right hand sides of these equations gives the equation through the center inflection point (cf. Fig. 3), which can also be found by using the second part of Eq. (11) with $\partial^2 U/\partial K_e^2 = 0$.

For Eq. (16), the two terms on the right hand side are nearly equal and opposite. They almost cancel each other out so the estimation in Eq. (12) for the hyperpolarized branch remains accurate:

$$U_{hyp} \approx \tilde{U} + \ln\left(\frac{K_e^{h\to d}}{K_i}\right). \tag{18}$$

This implies that the snowballing from the hyperpolarized branch to the depolarized branch *will* occur after about half of the IRKs have closed. For the depolarized branch (Eq. (15)) the hyperbolic arccosine term presents another dependence on $K_e$ so an approximation will ease the analysis.

$$\begin{aligned}\varepsilon \operatorname{arccosh}(-G) &= \varepsilon \ln(-G - \sqrt{G^2 - 1}) \\ &= \varepsilon \ln\left(-G - G\sqrt{1 - \frac{1}{G^2}}\right) \approx \varepsilon \ln(-2G)\end{aligned} \tag{19}$$

The last step in Eq. (19) is acceptable because $G(K_e^{d\to h}) \approx -3.5$, so $1 \gg 1/G^2$. Furthermore, at $K_e^{d\to h}$ the potassium concentration is high enough to make the Michaelis–Menten term in Eq. (17) practically unity. With this approximation we end up with the depolarized potential:

$$\begin{aligned}U_{dep} = \tilde{U} &+ \ln\left(\frac{K_e^{d\to h}}{K_i}\right) + \varepsilon \ln\left(\frac{P_0 + P_{\mathrm{IRK}}^{\max}}{P_0}\right) \\ &+ \varepsilon \ln\left(-2 - \frac{2U_{\max} P_{\mathrm{Na}} P_{\mathrm{IRK}}^{\max}}{3\varepsilon P_0 (P_0 + P_{\mathrm{IRK}}^{\max})}\right).\end{aligned} \tag{20}$$

Because of the extra terms here, the critical fraction of IRKs that need to open in order to switch back to the hyperpolarized branch is not 1/2. The extra terms will make the argument of the exponent in Eq. (10) larger than zero, which makes the permeability very small. It follows that the depolarized-to-hyperpolarized transition will happen after only *very few* of the channels have opened. Now taking the difference in the depolarized and hyperpolarized potentials with some rearrangement gives the height of the bistable region:

$$\Delta U \approx \ln\left(\frac{K_e^{d\to h}}{K_e^{h\to d}}\right) + \varepsilon \ln\left(-2\frac{P_{\mathrm{IRK}}^{\max}}{P_0}\left(1 + \frac{P_{\mathrm{Na}} U_{\max}}{3\varepsilon P_0}\right)\right). \tag{21}$$

Using the parameters from Fig. 3 with $K_e^{h\to d} = 1.6\,\text{mM}$ and $K_e^{d\to h} = 1.95\,\text{mM}$ we get more than triple the rough estimate of $\Delta U = 0.20$ that we had before. The result $\Delta U = 0.73$ is close to the $\Delta U = 0.65$ that is obtained from the fit. Using the approximation of Eq. (14) and some rearrangement we obtain:

$$\Delta U \approx \left(\frac{\Delta K_e}{K_e^{avg}}\right) + \varepsilon \ln\left(2\frac{P_{\text{IRK}}^{\max}}{P_0}\left(\frac{k_p}{\varepsilon P_0 C} - 1\right)\right). \tag{22}$$

It should be immediately obvious with Eq. (22) that with the aforementioned *Ansatz* of $\varepsilon \to 0$ the steepness of the transition increases and we again get the approximation of Eq. (14). Eq. (22) shows how the parameters affect the geometry of the bistable area, but does not tell the full story. As the parameters $\varepsilon$, $k_p$, $C$, $P_{\text{IRK}}^{\max}$ and $P_0$ are changed, the height and the position of the bistable area are also affected through the dependence of $K_e^{avg}$ on $\varepsilon$, $k_p$, $C$, $P_{\text{IRK}}^{\max}$ and $P_0$. The validity of Eq. (22) as an approximation can be tested by numerically checking (against Eq. (11) in conjunction with Eq. (10)) the geometry of the region. Upon plotting solutions we indeed see that a smaller $k_p$ leads to a shift of the bistable area to larger values of $K_e^{avg}$. This makes sense, as with less pumping capability, the cell will have to switch sooner to a depolarized state (the switch occurs when active transport cannot handle the extra sodium leak that hyperpolarization involves). A shift in the opposite direction (towards smaller $K_e^{avg}$) occurs when decreasing the osmolarity, $C$. Because $C = K_e + N_e \approx N_e$, decreasing $C$ effectively decreases $N_e$. A smaller $N_e$ reduces the sodium inflow (cf. Eq. (1)) and therefore presents less pressure on the pump. Increasing $P_0$ has the same effect as adding some isoprenaline to the system. $P_0$ accounts for the permeability of all $K^+$ channels other than the IRKs, so increasing this value is analogous to opening more $K^+$ channels that, unlike the IRKs, remain open at low $K_e$ values. Increasing $P_0$ has the effect of decreasing the height and width of the bistable region. It can be seen in Eq. (22) that with a sufficiently large $P_0$, a sufficiently large $C$ or a sufficiently small $k_p$ the logarithm will eventually give an imaginary number. The expression is then meaningless, $\Delta U$ is effectively undefined, and we no longer have hysteresis. All in all, Eq. (22) describes how for finite parameter values a bifurcation occurs; a bistable region appears or disappears.

## 6. Results and Discussion

We have studied the maintenance of the ionic balance of a living cell. Our simple model involved only sodium and potassium. Active transport in our model against the electrochemical potential is carried out solely by the Na,K-ATPase. Passive transport takes place through sodium and potassium channels. We have shown that hysteretic behavior of the membrane potential emerges when the potassium permeability is not fixed and constant, but made to depend on the electrochemical potential of potassium (cf. Eq. (10)). Our experiments with muscle cells give good agreement with the results of the analysis of the model. Fig. 1 depicts the theory and experiment for the case of a large constant potassium permeability. Fig. 2 shows how a potassium permeability that is dominated by the IRKs (which have an open probability that depends on the electrochemical potential of potassium) leads to a bistable area. For this case, experiment and theory show first order phase transitions and hysteresis. Approximations that are inferred from the model can quantitatively account for how the dimensions and the location of the bistable area depend on the different parameters of the model.

Though our experiments were performed on muscle cells, this phenomenon is seen in other types of cells (Gadsby and Cranefield, 1977; McCullough et al., 1990; Siegenbeek van Heukelom, 1991; Brismar and Collins, 1993; Jiang et al., 2001). Our analysis may shed light on the broader issue of the role of IRKs in the potassium permeability of all cells. In the last chapter of the well-known textbook by Hille (1992) the evolution of ion channels is reconstructed. Extrapolating three billion years into Earth's past is speculative. However, it is in the context of early evolution that we should be looking for an explanation of the bistability. On the basis of sequence homologies Hille estimates that IRKs first emerged more than 2400 million years ago. Hille suggests that there was a transitional period occurring 2000–3000 million years ago during which many traits evolved to give way for the eukaryotic cell to develop. IRKs may be considered evolutionarily ancient and are found in both eukaryotes and prokaryotes (Miller, 2000; Durrell and Guy, 2001).

The selective advantage of the switch discussed in this article is that it enables the cell to shut down in conditions of environmental stress. In the depolarized state the cell is insulating itself from the environment. With ion channels mostly closed and a very small electric transmembrane potential, ion leak will be minimal. Consequently, the Na,K-ATPase pumps need not operate at a high turnover rate and ATP consumption will thus be very low. The sharp decrease of the transmembrane electric potential $U$ that we see in Fig. 1 could already qualify as a kind of switch. However, a switch without a bistable region carries the disadvantage that a cell can repeatedly "go to sleep" and "wake up" if the extracellular potassium concentration were to fluctuate in the $K_e < K_e^*$ region. No such metabolic confusion occurs if there is a sufficiently wide bistable region. A hyperpolarized to depolarized transition takes place when $K_e < K_e^{h\to d}$. The cell will remain in its state of hibernation also when $K_e$ will subsequently fluctuate around $K_e^{h\to d}$. Only when $K_e$ is large enough that the cell will not be metabolically compromised does the cell "wake up." In the same respect, fluctuations of $K_e$ around $K_e^{d\to h}$ will not lead to a switch once the cell is "awake". The first order phase transitions and the bistable region provide the cell with a very robust safeguard against environmental challenge.

The role of chloride was not considered in this model. Chloride is important in the regulation of the transmembrane potential and volume homeostasis. The permeability for $Cl^-$ can be up to an order of magnitude higher than the permeability of $K^+$ (Bretag, 1987). Like for $K^+$, for $Cl^-$ at physiological conditions the electric and chemical potentials nearly balance. The Na,K,2Cl-cotransporter is driven by inward $Na^+$ flow and therefore leads to a greater sodium leak and a slight accumulation of intracellular $Cl^-$ above the equilibrium value. Changing the flux of $Cl^-$ by stimulating or blocking the Na,K,2Cl-cotransporter preserves the hysteresis, but has effects on $K_e^{avg}$, $\Delta K_e$, and/or $\Delta U$ (Gallaher et al., 2009). Blocking the Na,K,2Cl-cotransporter effectively leads to a lower $K_e^{avg}$ and a higher $\Delta U$, whereas stimulating the Na,K,2Cl-cotransporter leads to a higher $K_e^{avg}$, a lower $\Delta K_e$, and a slightly smaller $\Delta U$. Coupling $Na^+$ and $K^+$ transport to $Cl^-$ transport adds a complication to the system but appears to not change the basic dynamics. The effect of the chloride traffic on Eq. (22) may be as simple as adding another load on the pump and thereby decreasing the ratio $k_p/C$. However, the introduction of more adjustable parameters leads to larger equations and immunization of the theory against experimental falsification. By neglecting chloride we sacrifice the accuracy of parameter estimates for the sake of simplicity and conciseness.

The transmembrane potential is dependent on the permeability of potassium which is, in turn, dependent on the extracellular concentration of potassium and the transmembrane potential itself. This nonlinearity may result in either a hyperpolarization or a depolarization of the transmembrane potential at low $K_e$. For normal function, the extracellular concentration of potassium must lie within a certain range, but low potassium conditions do occur. This is referred to as hypokalemia and the condition most commonly results from excessive potassium loss via the kidney associated with the long-term use of diuretics. In extreme circumstances, hypokalemic patients can have temporary paralysis, which may be due to muscle cells switching to a depolarized state. The

most common treatment for hypokalemia is through potassium supplementation, though this often is overshot leaving one with hyperkalemia. Getting a good grip on the location and dimensions of the hysteretic region should be helpful in both understanding and treating this condition.

## References


Bretag, A., 1987. Muscle chloride channels. Physiological Reviews 67, 618–724.

Brismar, T., Collins, V.P., 1993. Effect of external cation concentration and metabolic inhibitors on membrane potential of human glial cells. Journal of Physiology 460, 365–383.

Costa, P., Emilio, M., Fernandes, P., 1989. Determination of ionic permeability coefficients of the plasma membrane of *Xenopus laevis* oocytes under voltage clamp. The Journal of Physiology 413, 199–211.

Durrell, S.R., Guy, H.R., 2001. A family of putative kir potassium channels in prokaryotes. BMC Evolutionary Biology 1, 1–14.

Edelstein-Keshet, L., 1988. Mathematical models in biology. In: Birkäuser Mathematics Series. McGraw-Hill Inc., New York.

Ferrell, J.E., Machleder, E.M., 1998. The biochemical basis of an all-or-none cell fate switch in xenopus oocytes. Science 280, 895–898.

Gadsby, D.C., Cranefield, P.F., 1977. Two levels of resting potential in cardiac purkinje fibers. The Journal of General Physiology 70, 725–746.

Gallaher, J., Bier, M., Siegenbeek van Heukelom, J., 2009. The role of chloride transport in the control of the membrane potential in skeletal muscle-theory and experiment. Biophysical Chemistry 143, 18–25.

Geukes Foppen, R.J., Siegenbeek van Heukelom, J., 2003. Isoprenaline-stimulated differential adrenergic response of $K^+$ channels in skeletal muscle under hypokalaemic conditions. Pflügers Archiv European Journal of Physiology 446, 239–247.

Geukes Foppen, R.J., van Mil, H.G.J., Siegenbeek van Heukelom, J., 2003. Effects of chloride transport on bistable behaviour of the membrane potential in mouse skeletal muscle. The Journal of Physiology 542, 181–191.

Geukes Foppen, R.J., 2004. In skeletal muscle the relaxation of the resting membrane potential induced by $K^+$ permeability changes depends on $Cl^-$ transport. Pflügers Archiv 447, 416–425.

Goodman, M.B., Art, J.J., 1996. Positive feedback by a potassium-selective inward rectifier enhances tuning in vertebrate hair cells. Biophysical Journal 71, 430–442.

Guo, D., Lu, Z., 2003. Interaction mechanisms between polyamines and irk1 inward rectifier $K^+$ channels. Journal of General Physiology 122, 485–500.

Hagiwara, S., Takahashi, K., 1974. The anomalous rectification and cation selectivity of the membrane of a starfish egg cell. Journal of Membrane Biology 18, 61–80.

Hille, B., 1992. Ionic Channels in Excitable Membranes. Sinauer Associates Inc., Sunderland, MA.

Jackson, E.A., 1989. Perspectives of Nonlinear Dynamics. Cambridge University Press, Cambridge, UK.

Jiang, Z., Si, J.Q., Lasarev, M.R., Nuttal, A.L., 2001. Two resting potential levels regulated by the inward-rectifier potassium channel in the guinea-pig spiral modiolar artery. Journal of Physiology 537, 829–842.

Katz, B., 1949. Les constantes électriques de la membrane du muscle. Archives des Sciences Physiologiques 3, 285–299.

Keener, J.P., Sneyd, J., 1998. Mathematical Physiology. Springer-Verlag, Berlin.

Kristensen, M., Hansen, T., Juel, C., 2006. Membrane proteins involved in potassium shifts during muscle activity and fatigue. American Journal of Physiology-Regulatory, Integrative and Comparative Physiology 290, R766–R772.

Kume, H., Takai, A., Tokuno, H., Tomita, T., 1989. Regulation of $Ca^{2+}$-dependent $K^+$-channel activity in tracheal myocytes by phosphorylation. Nature 341, 152–154.

Läuger, P., 1991. Electrogenic Ion Pumps. Sinauer Associates Inc., Sunderland, MA.

Lewis, K., 2007. Persister cells, dormancy and infectious disease. Nature Reviews Microbiology 5, 48–56.

Liu, J.-H., Bijlenga, P., Fischer-Lougheed, J., Occiodoro, T., Kaelin, A., Bader, C.R., Bernheim, L., 1998. Role of inward rectifier $K^+$ current and of hyperpolarization in human myoblast fusion. Journal of Physiology 510, 467–476.

Lu, Z., 2004. Mechanism of rectification in inward-rectifier $K^+$ channels. Annual Review of Physiology 66, 103–129.

McCullough, J.R., Chua, W.T., Rasmussen, H.H., Eick, R.E.T., Singer, D.H., 1990. Two stable levels of diastolic potential at physiological $K^+$ concentrations in human ventricular myocardial cells. Circulation Research 66, 191–201.

Miller, C., 2000. An overview of the potassium channel family. Genome Biology 1, 1–5.

Moore, W.J., 1972. Physical Chemistry. Prentice Hall Inc., Englewood Cliffs, NJ.

Murray, J.D., 1993. Mathematical Biology. Springer-Verlag, Berlin.

Plischke, M., Bergersen, B., 1994. Equilibrium Statistical Physics. World Scientific Publishing, Singapore.

Qian, H., Reluga, T.C., 2005. Nonequilibrium thermodynamics and nonlinear kinetics in a cellular signaling switch. Physical Review Letters 94, 028101-1–028101-4.

Reichl, L.E., 1980. A Modern Course in Statistical Physics. University of Texas Press, Austin, TX.

Sejersted, O.M., 1988. Maintenance of Na, K-homeostasis by Na, K-pumps in striated muscle. Progress in Clinical and Biological Research 268B, 195–206.

Sejersted, O., Sjøgaard, G., 2000. Dynamics and consequences of potassium shifts in skeletal muscle and heart during exercise. Physiological Reviews 80, 1411–1481.

Siegenbeek van Heukelom, J., 1991. Role of the anomalous rectifier in determining membrane potentials of mouse muscle fibres at low extracellular $K^+$. The Journal of Physiology 434, 549–560.

Siegenbeek van Heukelom, J., 1994. The role of the potassium inward rectifier in defining cell membrane potentials in low potassium media, analyzed by computer simulation. Biophysical Chemistry 50, 345–360.

Sims, S.M., Kelly, M.E., Dixon, S.J., 1991. $K^+$ and $Cl^-$ currents in freshly isolated rat osteoclasts. Pflügers Archiv 419, 358–370.

Sonenshein, A.L., 2000. Control of sporulation initiation in *Bacillus subtilis*. Current Opinion in Microbiology 3, 561–566.

Stadnicka, A., Bosnjak, Z.J., Kampine, J.P., Kwok, W.-M., 2000. Modulation of cardiac inward rectifier $K^+$ current by halothane and isoflurane. Anesthesia & Analgesia 90, 824–833.

Standen, N.B., Stanfield, P.R., 1978. Inward rectification in skeletal muscle: a blocking particle model. Pflügers Archiv 378, 173–178.

Struyk, A.F., Cannon, S.C., 2008. Paradoxical depolarization of $Ba^{2+}$- treated muscle exposed to low extracellular $K^+$: insights into resting potential abnormalities in hypokalemic paralysis. Muscle and Nerve 37, 326–337.

van Mil, H.G.J., Geukes Foppen, R.J., Siegenbeek van Heukelom, J., 1997. The influence of bumetanide on the membrane potential of mouse skeletal muscle cells in isotonic and hypertonic media. British Journal of Pharmacology 120, 39–44.

van Mil, H.G.J., Siegenbeek van Heukelom, J., Bier, M., 2003. A bistable membrane potential at low extracellular potassium concentration. Biophysical Chemistry 106, 15–21.

Wharton, D.A., 2002. Life at the Limits: Organisms in Extreme Environments. Cambridge University Press, Cambridge, UK.

Yang, J., Jan, Y.N., Jan, L.Y., 1995. Control of rectification and permeation by residues in two distinct domains in an inward rectifier $K^+$ channel. Neuron 14, 1047–1054.

Yan, D., Nishimura, K., Yoshida, K., Nakahira, K., Ehara, T., Igarashi, K., Ishihara, K., 2005. Different intracellular polyamine concentrations underlie the difference in the inward rectifier $K^+$ currents in atria and ventricles of the guinea-pig heart. The Journal of Physiology 563, 713–724.